Analyses of Surface Relief Gratings Inscription in Epoxy-Azo Linear and Crosslinked Polymers

Antonela B. Orofino, María J. Galante, Patricia A. Oyanguren

Grupo de Polímeros Nanoestructurados (PolNano), Instituto de Investigación en Ciencia y Tecnología de Materiales (INTEMA), Universidad Nacional de Mar del Plata (UNMdP), Consejo Nacional de Investigaciones Científicas y Técnicas (CONICET), Mar del Plata, Buenos Aires, Argentina
Correspondence to: A. B. Orofino (E-mail: aorofino@fi.mdp.edu.ar)

Received 30 March 2017; accepted 14 July 2017; published online 00 Month 2017
DOI: 10.1002/polb.24411

ABSTRACT: This work evaluates the inscription of surface relief gratings (SRG) in a series of epoxy-azo prepolymers and networks, both based on the same azo chromophore. Variables such as matrix structure (thermoplastic/thermoset), film thickness, exposure time, power of the incident laser beam, and content of azobenzene were analyzed on the final modulation depth of the gratings. The main goal of the article is to achieve the efficient formation of SRGs on crosslinked azopolymer films in a single step, in a reasonable time, and to a significant extent. The progressive erasure of the obtained structures with increasing temperature showed that part of the photoinduced information remained encoded in the material: as the relief partially relaxed above the glass transition temperature of the bulk material (116 °C) and up to 200 °C, its modulation remained in about one third of the initial height, and did not completely disappear. © 2017 Wiley Periodicals, Inc. J. Polym. Sci., Part B: Polym. Phys. **2017**, *00*, 000–000

KEYWORDS: azo polymers; crosslinking; epoxy networks; surface relief gratings; templates

INTRODUCTION It has been 30 years since research on light-induced molecular control in photoresponsive azobenzene-containing polymer films started receiving greater interest due to their potential use in photonic applications.[1–4] Optical data storage, holography, optical switching, display technology, micro/nanopatterning, and optical-to-mechanical energy conversion were among the uses of these material systems, responding to the changing times and needs.[5–10]

Azobenzene molecules exhibit numerous photoresponsive features that can be exploited in the design of functional materials to locally modify their properties. Specifically, the irradiation of azobenzenes with polarized light results in a fast and efficient photoselective isomerization, accompanied by a chromophore motion and alignment. If the azobenzene moieties are bound to a polymer chain, the extent of the photoinduced molecular motion can translate into larger scale motions, and even into macroscopic movements of the material system.[11]

One of the most remarkable photoresponsive effects in azopolymer systems is the formation of surface relief gratings (SRGS) on a thin film when exposed to an incident light pattern. This modulated surface deformations or topographic patterns reflect the state of the incident light polarization and the light intensity distribution on the material through an all-optical photoinduced mass transport.

Several mechanisms have been proposed to explain the origin of the driving force for SRG inscription,[12,13] but none of them has successfully managed to give a full and proper explanation. Recently, Sekkat[14] developed a theoretical model that describes photomigration as a phenomenon based on a *photoisomerization force*, that requires the existence of a polarization-dependent gradient of light intensity and a photochemical phenomenon, for example, photoisomerization to trigger molecular motion.

This single-step, reversible, light-induced surface modulation process, along with the critical factors that determine it, have been extensively studied since its emergence.[5,15,16] SRG generation allows to obtain easily controllable periodic micro and nanostructures over a considerable area in a very simple way at room temperature and under moderate intensity irradiation (1–100 mW cm^{-2}). This technique offers a huge potential for immediate applications in the fields of photofabrication and nanotechnology.[7–9]

The basic main application of these devices is optical.[5] They can be exploited for holographic image or data storage,[17] as

Additional Supporting Information may be found in the online version of this article.

optical polarizers,[18] angular wavelength filters,[19] or even couplers for optical devices.[20] Starting with a thin azopolymer layer, a wide variety of photonic elements can be created (diffraction gratings, microlens arrays, photonic crystals, plasmonic sensors, antireflection coatings, and nanostructured light-polarization converters), either by using the patterned films directly or by using them as templates, molds, and etching masks for the fast and cost-effective periodic structuring of other materials.[8,9]

While in some cases, the reversibility in the formation of microstructures is of particular interest, for optical components, the optical properties must be invariant over time. An important requisite of SRG is shape stability for long-term storage and durability at higher temperatures.

Reliefs stability can be improved using high glass transition temperature (T_g) amorphous polymers, although these materials lack the fluidity necessary for mass migration, and the process is inefficient due to the rigidity of the chains.[21,22] The same effect is noticed when the molecular weight of the polymer is increased.[23,24] In this case, the physical links of the chains (*entanglements*) could act as crosslinking points, thereby restraining the molecular motion for grating formation. Another permanent fixation strategy is to generate the relief on the first place, followed by a subsequent photochemical or reaction crosslinking step.[25–27] However, this technique is often poorly reproducible and the reliefs do not keep their initial quality. An important goal to achieve would be the efficient formation of SRG directly from crosslinked polymers in a single step, in a reasonable time, and to a significant extent.

Few examples in the literature reveal a direct SRG inscription on crosslinked systems in which small modulations (<30 nm) are obtained, since molecular motion on a large scale seems to be prevented in the network structure.[27,28] The authors have successfully generated SRG on thermoset samples.[29,30] The exposure conditions were tested and optimized in different polymeric systems to find a way to inscript permanent SRGs on crosslinked polymers, obtaining interesting modulations in a reasonable time.

Based on the above, a thermoplastic azo-prepolymer was used in the first part of this study to evaluate SRG formation. In the second part, the generation of SRG was assessed in crosslinked samples of different thicknesses obtained from a complete series of azo-prepolymers, which differed in their composition, that is, azobenzene content.

EXPERIMENTAL

Materials and Sample Preparation

Azopolymers: Synthesis and Film Deposition

An azo chromophore 4-(4′-nitrophenylazo) aniline [Disperse Orange 3 (DO3), Aldrich, dye content 95%, $T_m = 200$ °C] was selected as the photosensitive monomer. This is a *pseudostilbene* or *push-pull* type of azomolecule, where the 4- and 4′-position electron-donating and electron-withdrawing groups

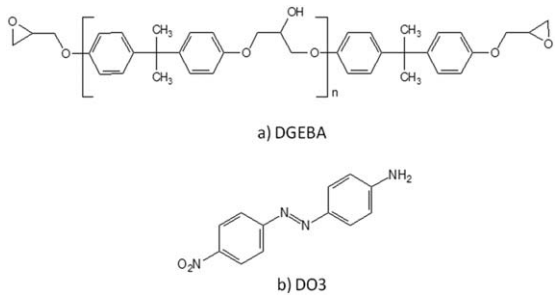

FIGURE 1 Chemical structure of the materials: DGEBA and DO3.

lead to a large molecular dipole, inherent nonlinear optical properties, and other highly-efficient photophysical effects. The difunctional epoxy resin used was diglycidyl ether of bisphenol A (DGEBA, DER 332, Sigma-Aldrich) with a mass per mol of epoxy groups equal to 174 g mol^{-1}. Their chemical structures are shown in Figure 1.

The amino group functionality in the chromophore can be reacted with the epoxy groups to straightforwardly obtain azo-modified linear and crosslinked polymers. A series of azo-containing epoxy precursors was synthesized by the bulk reaction of DO3 and DGEBA, varying the amine/epoxy stoichiometric ratio $r = (0.25–1)$. Reaction mixtures were prepared by mixing the monomers and cured to obtain soluble products (first stage). The reaction details and the characterization of the resulting materials have already been studied and reported.[29]

The precursors obtained after the first stage were dissolved in tetrahydrofuran (Biopack, 99%) at a concentration of 2–10 wt %, and then filtered. Films were prepared by spin-coating the solutions over previously cleaned glass slides, using a single wafer spin processor (WS-400E-6NPP-lite, Laurell Technologies Corp.), and a spinner cycle program of 3000 rpm for 60 s. Samples were subsequently dried in a vacuum chamber for 24 h to remove residual solvent, and then stored at room temperature. Film thicknesses (d) were varied (in a range of 100–1500 nm) by adjusting the concentration of the solution. They were measured by profilometry (KLA Tencor D100 mechanical profilometer), sensing the height difference between the film and the glass substrate across a scratch made on the sample.

To obtain azo-networks, the samples prepared as specified above were subjected to thermal treatment in a convection oven during the time necessary for each formulation to attain complete conversion of epoxy monomer (second stage of curing).[29]

Inscription of SRGs

SRG generation was performed using a Lloyd mirror interferometer in the standard experimental setup, combined with a semiconductor laser at 488 nm (Coherent Sapphire 488–20 OEM Laser), whose wavelength coincided with the maximum absorbance of the chromophore. The laser beam was

expanded and collimated with the addition of a divergent lens in its optical path.

The interferometer basically consists of a mirror placed normal (perpendicular) to a glass slide where the sample is deposited. This is a widely used setup for the generation of fringe patterns from a coherent source.[31] The apparatus and its configuration are simple, versatile, and stable. An interference pattern is projected onto the polymer film by the combination of one half of the incident laser beam and the other half beam that is reflected back from the mirror, coincident with the direct beam.

The fringe spacing Λ is easily controlled by varying the incidence angle,whose estimation can be calculated from

$$\Lambda = \lambda/(2 \sin \theta) \quad (1)$$

where λ is the writing laser wavelength, and θ is the angle between the beam propagation axis and the normal direction of the sample (plane parallel to the mirror). In this work, the first series of SRGs inscribed on polymer films (azo-prepolymers and azo-networks) was obtained using an experimental setup for which the resulting period or spacing between peaks was approximately 2 μm ($\theta = 7°$). The second set of samples was prepared for the analysis of SRG inscription on different compositions (i.e., variation in azo content). In that particular case, the angle was slightly modified ($\theta = 5°$), leading to a 2.8-μm period between peaks.

The polarization state of the system was orthogonal linear with the polarization planes at an angle of 45° with respect to the incidence plane (+45°: −45°), for being one of the most efficient conditions for grating generation (higher amplitude h of the inscribed SRG).[32]

For all the measurements, the laser beam power was varied between 8 and 12 mW, incident over a semicircular area of 4 mm diameter (equivalent to 130 and 190 mW cm^{-2}, respectively, reported as irradiance units). Those values represent 40–60% of the laser beam maximum power (20 mW). All the experiments were conducted at room temperature (18–20 °C).

Characterization Techniques

Differential scanning calorimetry (Pyris 1 Perkin Elmer) was used to determine thermal transitions of azo-prepolymers and azo-networks. Dynamic scans were carried out under nitrogen flow at 10 °C min^{-1}, and the T_g was defined at the onset of the change in specific heat. Reported values correspond to the first heating scan in all the cases.

Confocal Raman microspectroscopy (CRM) was used to assess the extent of any possible photodegradation after irradiation with the laser writing beam, used for SRG generation. Raman spectra were recorded with a Renishaw Reflex InVia spectrometer, equipped with a CCD detector of 1040 × 256 pixels, and coupled with a Leica optical confocal microscope with a computer-controlled *x–y–z* motorized stage.

Spectra were acquired under a ×100 objective, with an exposure time of 2 sec, averaging 5 accumulations, by impinging 10% laser power of a laser line (785 nm, 300 mW), used as an excitation source in combination with a grating of 2400 grooves mm^{-1}. The spectral resolution was 4 cm^{-1}. In some cases, spectra were taken under identical conditions though in a high confocality mode to enhance the signal and reduce the contribution of the glass substrate. The laser power was kept low to avoid sample damage, while keeping good spectra quality. The effective power of the laser impinging on the sample under these conditions (10% of incident beam power) was 7 mW for ×50 objective and 3 mW for ×100 (measured punctually on the irradiated area). The optical microscope was used to register micrographies of the samples surface (×50–×100 objective).

The morphologies of the generated SRG were observed and characterized by atomic force microscopy (AFM). An Agilent Technologies' SPM 5500 scanning probe microscope was used, working in intermittent contact or *tapping* contact mode, at a scan rate between 1 and 2 lines s^{-1}, simultaneously obtaining images of topography, amplitude and phase differences (10 μm × 10 μm–20 μm × 20 μm areas). AFM operation in tapping mode is key to eliminate films mechanical deformation by the cantilever. Unless otherwise indicated, the images were taken at room temperature, keeping relative humidity below 40%.

The thermal stability of the gratings was evaluated by AFM as well, using a heating chamber with temperature control (from room temperature to 250 °C) to thermostatize the sample and monitor the amplitude of the reliefs *in situ*, once subjected to the heating program. Temperature rise was determined at a heating rate of 10 °C min^{-1}, allowing the system to stabilize for 2 min after reaching the desired temperature before scanning. The remaining parameters were maintained as described above, as this accessory allows the scanning probe to work in normal conditions and regular configuration.

The modulation depth and the spacing between peaks of the inscribed SRGs were determined as an average of five equally spaced transverse cross-section scans of two micrographs for each sample. The reported associated error for each data series is the calculated standard deviation.

RESULTS AND DISCUSSION

Part A: Azo-Prepolymers

In this section, the results corresponding to thermoplastic azo-polymers are compared with those of the crosslinked series, for having the same composition, although different molecular structure. To begin with, the maximum intensity modulation obtained in a certain time frame for films of different thicknesses of the same azo-prepolymer ($r = 0.5$; $T_g = 24$ °C) was analyzed.

The irradiation power was set at 130 mW cm^{-2}, and exposure times were arbitrarily chosen as 30, 45, and 60 min. In

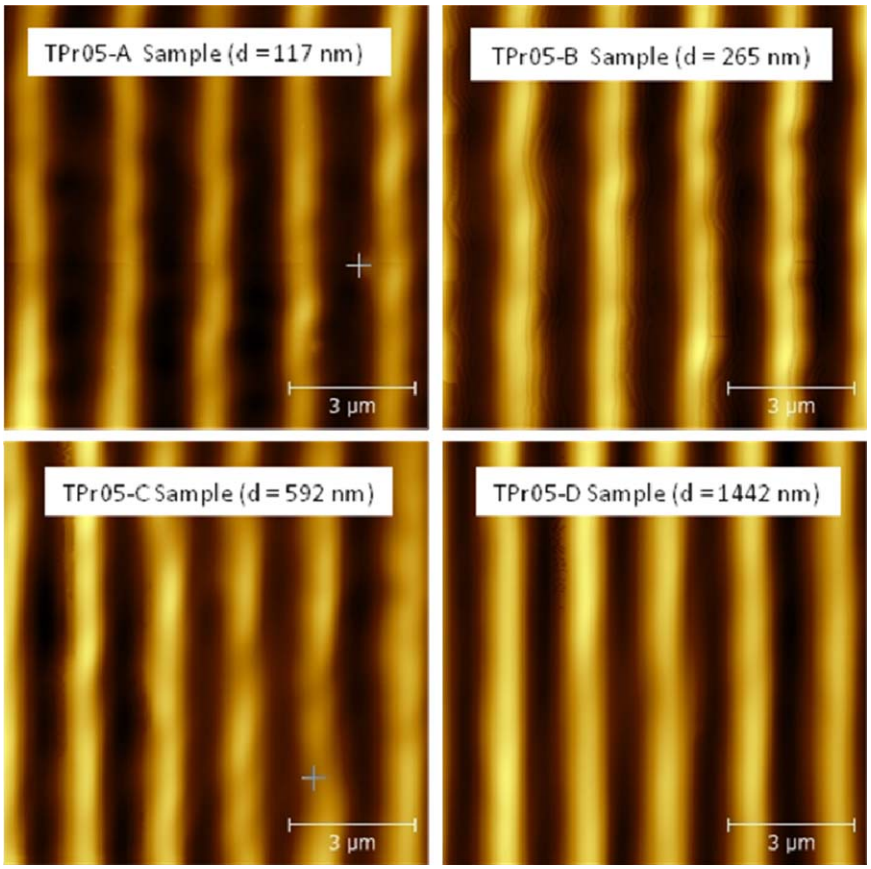

FIGURE 2 AFM topographic images of SRG inscribed on azo-prepolymer films under identical exposure conditions and different film thicknesses (laser beam power: 130 mW cm^{-2}; exposure time: 60 min). [Color figure can be viewed at wileyonlinelibrary.com]

this case, the reliefs were easily formed in a reasonable time and could be noticed by the mere observation of the samples (litmus type areas), as they work as diffraction gratings, decomposing white light into its components. Efficient SRG formation on similar epoxy-based low molecular weight azo-polymer films has already been demonstrated.[33]

The topographic images of the SRGs obtained after the longest exposure time are presented in Figure 2. All the gratings obtained are of very good quality, showing a regular and periodic modulation of well-defined and parallel valleys and crests. The results obtained for films of different thicknesses are displayed in Figure 3. The relative height of the relief (h_R) was also calculated as the ratio between the maximum amplitude and film thickness (Table 1). This parameter can be related to the fraction of the total mass that has been mobilized during the relief inscription.

During grating inscription, as the irradiation time increases, the height of the corresponding SRG increases monotonically as well in all samples, tending toward a saturation modulation value. This feature is commonly observed, with irradiation intensities ranging from 5 to 200 mW cm^{-2} and the same grating height at saturation, although SRG formation rate increases with laser power.[23] Under these conditions of moderate irradiation, the efficiency of the relief formation depends only on the net irradiation dose. As it can be noticed in Table 1, under the same net exposure (identical irradiation time under the same laser power), thicker films showed enhanced modulation. This may indicate that the

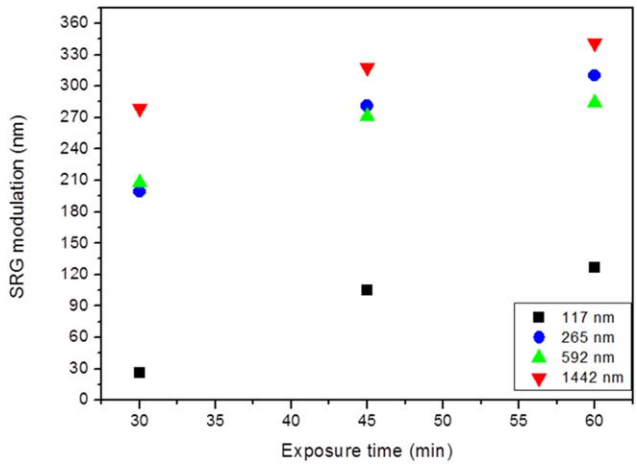

FIGURE 3 SRG modulation of azo-prepolymer films as a function of irradiation time and sample thickness (laser beam power: 130 mW cm^{-2}). [Color figure can be viewed at wileyonlinelibrary.com]

TABLE 1 Summary of SRG Properties for Azo-Prepolymers and Azo-Networks (Composition $r = 0.5$)

Sample ID	Film thickness d (nm)	SRG amplitude, $t = 30$ min (nm)	SRG amplitude, $t = 45$ min (nm)	SRG amplitude, $t = 60$ min (nm)	Relative height (h_R)
TPr05-A	117 ± 6	26 ± 3	105 ± 7	127 ± 9	1.09
TPr05-B	265 ± 8	199 ± 8	281 ± 10	310 ± 11	1.17
TPr05-C	592 ± 11	208 ± 11	271 ± 14	284 ± 8	0.48
TPr05-D	1442 ± 19	279 ± 12	318 ± 17	341 ± 12	0.24
Sample ID	Film thickness d (nm)	SRG amplitude, 130 mW cm^{-2}	SRG amplitude, 160 mW cm^{-2}	SRG amplitude, 190 mW cm^{-2}	Relative height (h_R)
TRr05-A	83 ± 5	Not formed	Not formed	Not formed	-
TRr05-B	176 ± 7	Not formed	$2{,}8 \pm 0{,}6$	$6{,}6 \pm 0{,}8$	0.04
TRr05-C	550 ± 11	16 ± 2	37 ± 4	38 ± 5	0.07
TRr05-D	1255 ± 14	46 ± 3	54 ± 4	56 ± 5	0.04

Note: For azo-prepolymer films: laser beam power: 130 mW cm^{-2}. For azo-network films: exposure time: 1 h.

driving force for the mobility of the polymer chains can be related to the sample total thickness.

Grating formation requires a significant mobility of the polymer chains[32,34,35] (at least locally and at a segmental level) to allow for rearrangement, especially at the surface level, in the upper layer whose thickness is around 2–20 nm. In a polymer film, at least three different layers can be distinguished within its thickness: an interfacial layer in direct contact with the substrate, a top surface layer in contact with air, and an intermediate "bulk" layer between them. The three zones are expected to be characterized by different molecular mobility of the polymer chains. While in the bottom interfacial layer mobility is restricted by the interaction due to direct contact with the substrate, the chains in the surface layer have good mobility and can easily change their conformation or diffuse on the surface. Thicker films have a larger proportion of molecules constituting the surface and the intermediate layers. As a consequence, faster structural rearrangements are expected in such films, as it was experimentally observed.

Kulikovska et al.[34], studied the formation of SRG in several polyacrylic-backbone polymers with azobenzene pendant groups and reported how the modulation of surface profiles is affected by film thickness. Grating formation in very thin films becomes ineffective due to the suppression of the polymer motion in the substrate confined layers. Specifically, thin films (thickness below 100 nm) were characterized by not forming reliefs and maintaining a flat surface after being irradiated. Very similar results were obtained by Yager and Barrett on acrylate-based polymers,[35] which suggested the existence of a certain size scale of material motion required to achieve an efficient mass transport. On the other hand, for films thicker than 500 nm, no changes were observed in the gratings height, regardless of the film thickness (under the same exposure conditions). The saturation of SRG modulation depth should be expected with film thickness, as only the surface layer absorbs radiation and is likely to obtain enough mobility under light illumination. This fact suggests that when there are no restrictions with respect to the mass that can be mobilized, amplitude only depends on irradiation conditions (laser beam incident angle, power and polarization, exposure time). The same trend was observed in the system studied herein for a given exposure time at a given power. For films over 265 nm thick, the gratings reached a saturation modulation value (300 nm).

The relative height of the relief was calculated (h_R) in the analyzed samples. This parameter allows to compare SRG in films of different thicknesses. In theory, the maximum modulation that can be obtained in a polymer film in an ideal case of complete mass transfer is twice its original thickness (relative relief height equal to 2). In practice, the relative grating height shows a maximum value indicating an optimal mass transfer. In thinner films, the process is hindered and in thicker ones h_R decreases as the modulation height saturates.

In this case, the observed trend is the one normally reported: the relative height of the thinner film (TPr05-A, $h_R = 1.09$; Table 1) is slightly smaller than that of the following, thereby indicating that the proportion of mobilized material is similar in both cases. However, as the maximum height of the relief is much lower than in the other cases, some extent of mass transfer hindrance can be deduced.

In fact, the obtained values of h_R above 1 are very satisfactory. In the referenced publications, Kulikovska et al. reported an optimum h/d ratio of around 0.17 (T_gs in the range of 77–135 °C), while Yager et al. reported maximum h_R values of about 0.55 (T_gs of around 100 °C). It is worth emphasizing that the azo-prepolymers synthesized here have a bulk T_g of 24 °C (onset). Despite such low T_gs, the obtained SRGs were stable at room temperature (*vide infra*). Viswanathan et al.[16] synthesized a low T_g azo-functionalized polymer with flexible alkyl chain backbone to study the effects of polymer chain mobility. The T_g of the polymer was about 35 °C. The authors noticed that even if photoinduced surface deformation was generated in this polymer, the deformation could not be fixed given the fairly high mobility of the

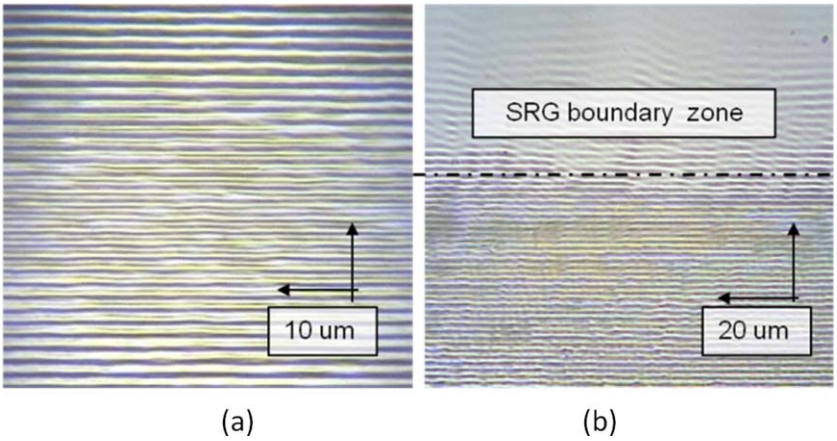

FIGURE 4 (a) Optical micrography (×100 magnification) of the SRG zone; (b) Optical micrography (×50 magnification) of the exposed/unexposed surface limit (TPr05-D sample, exposure time: 60 min). [Color figure can be viewed at wileyonlinelibrary.com]

polymer molecules near T_g, resulting in relaxation to a smooth surface due to surface tension forces. Probably the different behavior of both low T_g azopolymers was related to differences in the nature of the polymer main chain.

Degradation Assessment

The possible photodegradation of the azopolymer films was evaluated by CRM over the SRG irradiated area. Figure 4(a) shows the optical micrography inside the zone with the inscription of the surface relief for TPr05-D sample, subjected to the longest exposure time (60 min). A uniform pattern of dark and bright parallel lines can be clearly visualized. In Figure 4(b), the boundary of the SRG irradiated area (limit of exposed/unexposed surface) can be observed.

Raman spectra were recorded and analyzed on both zones, inside and outside the SRG inscription area to be compared for the assessment of photodegradation, as displayed in Figure 5.

Raman spectrum bands were assigned as follows: the peak at 1589 cm^{-1} corresponds to the phenyl ring, the peaks at 1445 and 1392 cm^{-1} to —N═N— stretching, and the peak at 1142 cm^{-1} corresponds to the phenyl-N stretching mode. Photodegradation is identified in this kind of films by the decrease in the characteristic peaks of the Raman signal of azobenzene, and by an increase in the background signal due to the chromophore degradation.[36,37] In this case, there are no significant variations between the spectra. Peaks do not practically differ in intensity or in frequency, thus indicating that no photodegradation of the polymer film occurred during SRG inscription.

Thermal Stability of the Reliefs

The thermal stability of the SRG generated in azoprepolymer films (TPr05-D sample; exposure time: 60 min) was evaluated by AFM, using the heating chamber to thermostatize the sample and monitor the modulation height of the relief *in situ*, as a heating program was applied. The profiles obtained and their average heights as a function of temperature are presented below in Figure 6(a,b).

Experimental results show that in the thermoplastic azopolymer films, a progressive erasure of the SRG was observed as temperature increased. This result was expected: reliefs are obtained from a reversible mass transport and the original flat surface can be recovered after heating above T_g, once the polymer chains are given enough mobility. At room temperature, the material is an amorphous glass and material movement is prevented. As temperature increases, the T_g is reached, the coordinated molecular motions are activated and the azo moieties recover a random configuration similar to the initial state. It is clear that, in amorphous systems, it is not possible to maintain photo-orientation above their T_g.

Experimentally, this phenomenon occurs at a temperature above 40 °C. The reported bulk T_g for the thermoplastic azopolymer (TPr05) is 24 °C. This corresponds to the onset of the transition, while the measured value at the endset for the same sample [Supporting Information Fig. S1(a,b)] can be found at around 35.5 °C. The dynamics of the polymer to rearrange during the heating program before recording the

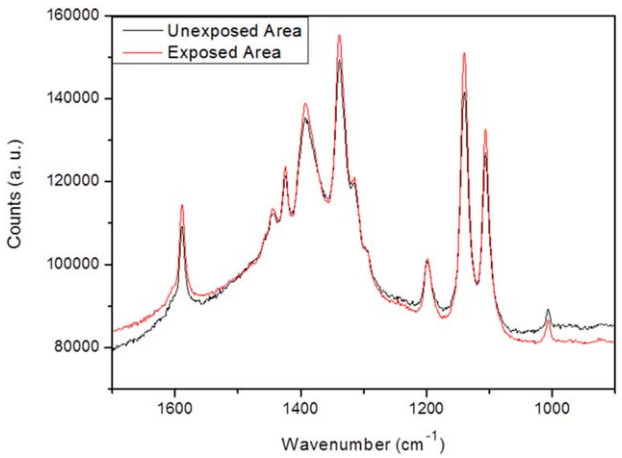

FIGURE 5 Raman spectra obtained from the unexposed and exposed (SRG) areas, (TPr05-D sample; exposure time: 60 min). [Color figure can be viewed at wileyonlinelibrary.com]

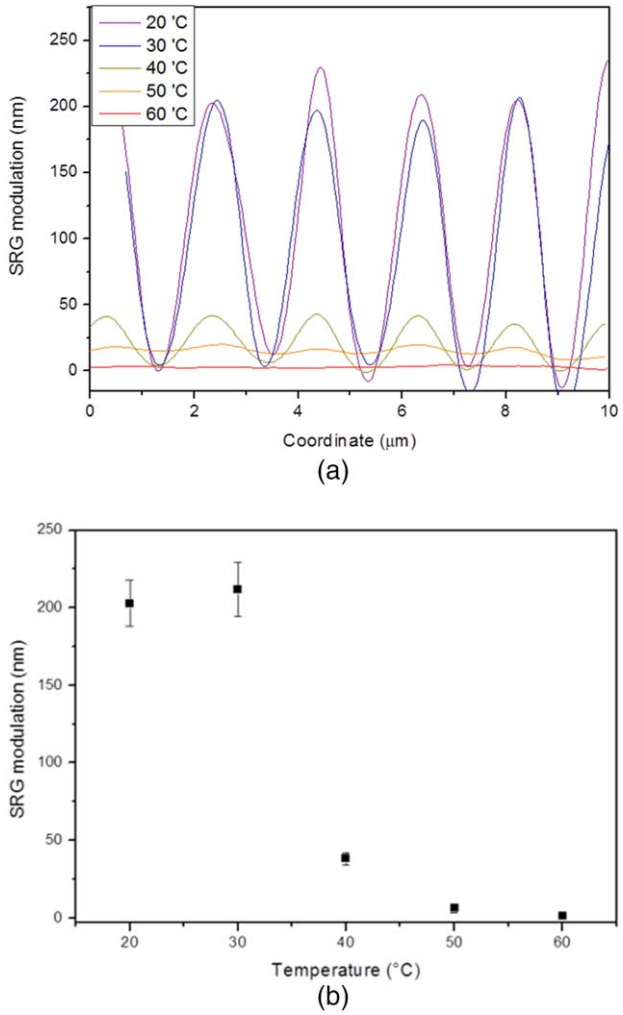

FIGURE 6 (a, b) SRG modulation (height profile) obtained by AFM as a function of temperature, recorded *in situ* under a heating program. [Color figure can be viewed at wileyonlinelibrary.com]

topographic image can also slightly affect the measured modulation at the glass transition. These facts may explain the easy formation and stability of gratings at room temperature.

Part B: Azo-Networks

As already stated, achieving the efficient formation of surface reliefs from crosslinked polymers in a single step would be an important goal. The authors have successfully generated SRGs on thermoset samples.[29,30] When performing preliminary tests for SRG inscription, it was discovered that the use of higher irradiation power and longer exposure time than that used for thermoplastic polymers allowed to obtain surface patterns on crosslinked polymers. The exposure conditions were tested and optimized on different polymeric systems to find a way to inscript permanent SRGs on crosslinked polymers, obtaining interesting modulations in a reasonable time.

Grating Formation

In this section, the study deals with SRG inscription on azo-networks of identical composition ($r = 0.5$) and different thicknesses. The irradiation power was set between 130 and 190 mW cm^{-2}, and the exposure time was arbitrarily set at 60 min. Figure 7 illustrates the topographic images obtained by AFM for samples irradiated with the maximum power used. The obtained results are summarized in Table 1 and Figure 8.

In the micrographs of the patterns formed, it can be observed, in the first place, that quality differs from that of thermoplastic azopolymers, although morphology remains clearly defined.

In addition, the formation of SRGs on azo-networks was satisfactory only in samples at least 550 nm thick. For thinner films, very small modulation profiles (sample TRr05-B) were observed, or no relief formation at all (sample TRr05-A).

In the light of the results obtained, an interpretation of polymer chain mobility in relation to film thickness similar to that developed for azo-prepolymers can be applied to the azo-networks. In this case, the existence of a critical thickness can be proposed, below which no SRG formation occurs. Grating modulation on very thin films is not effective, given the suppression of the molecular movement in the layers of the polymer film that can be considered confined by its proximity to the substrate.[32,34,35] In the case of polymer networks, large-scale polymer chain migration is further hindered by the crosslinked nature of the material, which makes the feasibility limit for SRG generation require greater thickness, and, at the same time, the obtained amplitudes are substantially lower.[27,28]

As regards power variation, the values obtained show a slight upward trend in the amplitude of the relief with increasing irradiation intensity. The behavior is consistent with the fact that both the rate of generation of the relief and the maximum modulation value are dependent on the power used, as observed in thermoplastic polymers.[23]

As a preliminary result, it was determined that the optimal conditions for SRG inscription on crosslinked films require at least one-micron thick samples, high power (around 200 mW cm^{-2}) and a minimum irradiation time of 1 h.

Degradation Assessment

Again the possible photodegradation of the azopolymer films was evaluated by CRM over the SRG irradiated area. Raman spectra were recorded for the samples subjected to the higher irradiation power (190 mW cm^{-2}) on the unexposed and exposed (SRG) areas, to evaluate the existence of photodegradation under the more drastic irradiation conditions.

In all the azo-networks analyzed, no changes were observed in the spectra, specially associated with a decrease in the band at 1142 cm^{-1} (phenyl-*N* stretch) characteristic of the azobenzene group degradation, inside and outside the SRG inscription area.

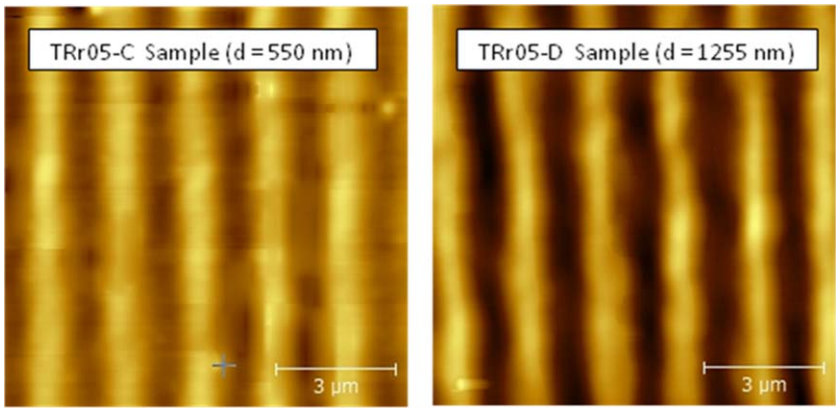

FIGURE 7 AFM topographic images of SRG inscribed on azo-network films, for identical exposure conditions and different film thicknesses (laser beam power: 190 mW cm^{-2}; exposure time: 60 min). [Color figure can be viewed at wileyonlinelibrary.com]

Based on the experimental evidence obtained, it was determined that the formation of surface reliefs on azo-networks did not lead to a noticeable photodegradation of the chromophore.

Azobenzene Content Variation

The chemical versatility of the epoxy-amine reactive system used permitted to synthetize a complete series of azo-networks of different composition with similar T_gs and bearing the same azo chromophore to evaluate SRG formation in crosslinked samples with different azobenzene content.

In this case, all the films were prepared with a final thickness of 1 μm, the writing power was set at 190 mW cm^{-2}, and the exposure time was arbitrarily chosen at 90 min. The topographic images obtained are shown in Figure 9, and the corresponding amplitudes and T_gs of the azo-networks are presented in Table 2.

As it can be seen from the topographic images in Figure 9 and from the data in Table 2, not every composition leads to the same quality and modulation depth of the inscribed SRGs in the series of azo-networks.

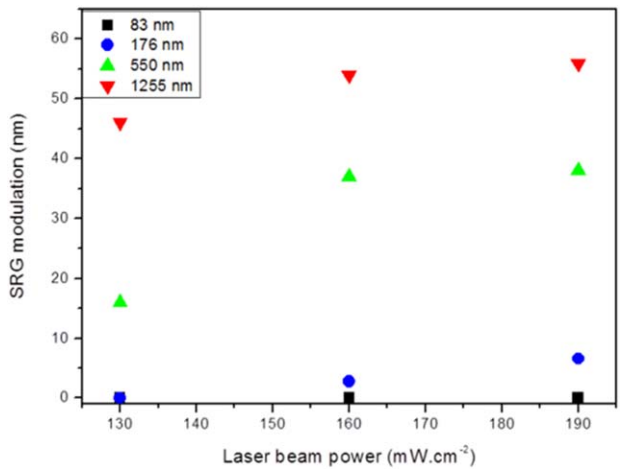

FIGURE 8 SRG modulation for azo-network films ($r = 0.5$) as a function of the laser beam power and film thickness (exposure time: 60 min). [Color figure can be viewed at wileyonlinelibrary.com]

A proportional linear trend between the modulation and content of azobenzene is observed, except for the TRr05 sample (25.8 wt % DO3) that presents a significantly greater maximum height. In the case of TRr025 and TRr1 samples, the shape of the grating is not as uniform as the ones obtained for the other two compositions. The results in this section suggest that the azo chromophore content and the network structure strongly influence the maximum SRG amplitude that can be obtained, as the optical setup and inscription conditions can be considered invariant.

On one hand, increasing the content of azo chromophore usually improves relief formation.[22] It is a fact that the repeated *trans-cis-trans* isomerization cycles of azobenzene moieties are necessary to allow material flow even well below its T_g. While it may seem that the mass transport phenomenon is purely superficial, it has been shown that every photoactive unit in the sample contributes to the phenomenon.[38]

On the other hand, as it was observed in linear systems, the bulkiness of the azo groups and thus the free volume requirements of the chromophores were found to affect the extent of the grating inscription process.[23,39] This is why the matrix properties take particular relevance, as the network structure and crosslink density determines the free volume and the mobility of the chains.

In this case, regarding TRr05 sample, the enhanced SRG height formation could be attributed to an optimal condition taking place in that composition, in which the combination of the studied factors results in an exceptional surface modulation. Laventure et al.[40] explained that the SRG potential of an azo-material depends on its capability to photo-orient and on the matrix properties. There is a compromise between the stability of grating formation and inscription kinetics. The matrix needs to have an adaptation capability to be pushed anisotropically during the azo isomerization, and to adapt to the redistribution of the azo moieties,

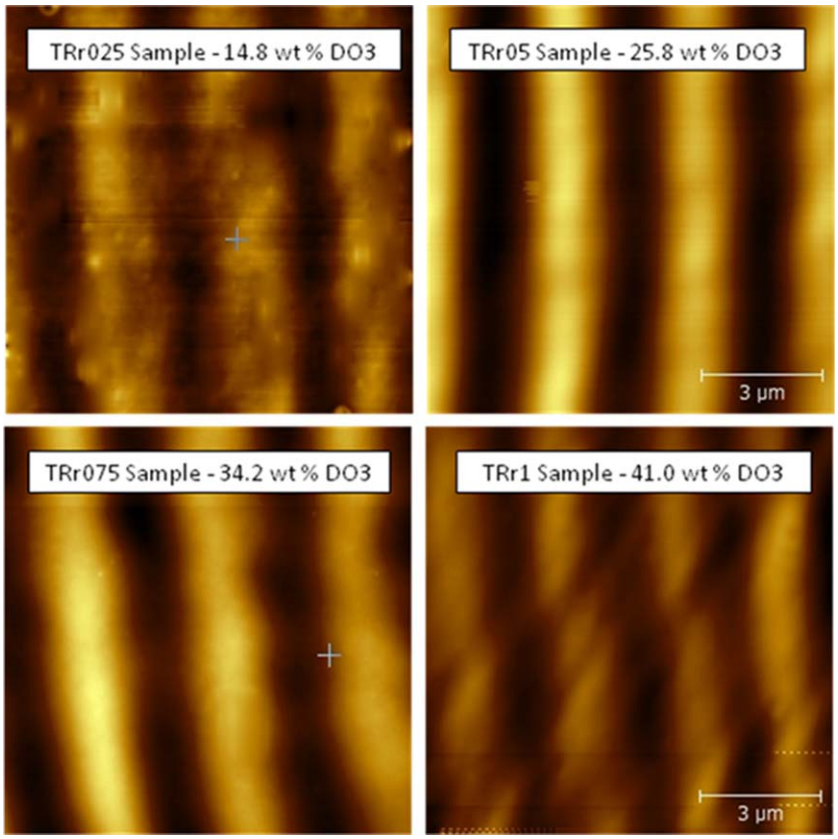

FIGURE 9 AFM topographic images of SRG inscribed on azo-networks under identical exposure conditions on films with different composition, that is, azo content (film thickness = 1 μm; laser beam power: 190 mW cm^{-2}; exposure time: 90 min). [Color figure can be viewed at wileyonlinelibrary.com]

maintaining the highest possible orientation, without exceeding a threshold to enable molecular motion.

If we analyze the reactions involved in the synthesis of the series of azo-networks, a step growth epoxy/amine reaction occurs in the first stage, and, in the second, crosslinking is achieved by chain growth polymerization of the epoxy units at the ends of the oligomers and hydroxyl groups. The different concentrations of DO3 lead to networks with different chemical structure, which is not that easy to determine. Further investigation should be conducted to achieve a better understanding of the processes involved. Even though the mechanism of formation of such reliefs is still unknown, a phenomenological analysis of the variables involved would be very useful to optimize the inscription process.

TABLE 2 Summary of SRG Properties of Azo-Networks with Different Composition (Azobenzene Content)

Sample ID	wt % DO3	SRG amplitude (nm)	T_g network (°C)
TRr025	14.8	15 ± 2	112
TRr05	25.8	123 ± 10	116
TRr075	34.2	45 ± 5	125
TRr1	41.0	57 ± 6	113

Note: film thickness = 1 μm; laser beam power: 190 mW cm^{-2}; exposure time: 90 min.

From the analysis above, it could be concluded that the formation of SRGs in azo-networks depends on film thickness, irradiation conditions, azo chromophore content, and, above all, on the three-dimensional network structure.

Thermal Stability of the Reliefs

Once the inscription of SRGs on azo-networks was satisfactorily achieved, their thermal stability and potential reversibility (thermal erasure) was evaluated by AFM.

The experiment was conducted on TRr05 sample ($r = 0.5$, $d = 1255$ nm, exposure time: 90 min), for which the best patterns were obtained, regarding both grating quality and the final height obtained, thus indicating that this composition is optimal for the inscription of SRG on easily-obtainable crosslinked films from a practical perspective. The obtained profiles as a function of temperature, along with the average height, are presented below in Figure 10(a,b).

In this case, the only significant variation in the modulation of the temperature relief function is observed when the film temperature exceeds the T_g of the bulk material [in this case $T_g = 116$ °C; the thermogram for the sample is shown in Supporting Information Fig. S1(c,d)]. Above this temperature,

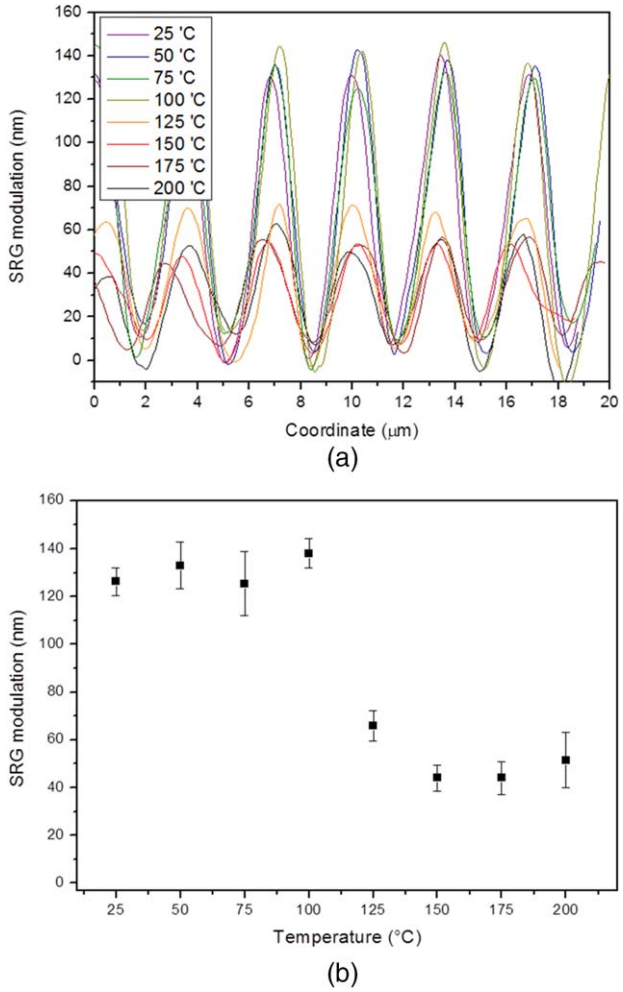

FIGURE 10 (a, b). SRG modulation (height profile) obtained by AFM as a function of temperature, recorded *in situ* under a heating program. [Color figure can be viewed at wileyonlinelibrary.com]

and up to 200 °C, the relief modulation remains at about one third of the initial height, and does not completely disappear.

The presence of crosslinking points restricts the free movement of the polymer chains still above T_g, maintaining part of the information encoded in the film. The films present some degree of lasting deformation, or reorganization of their structure when subjected to laser irradiation. This behavior is completely different from what has been reported for non-crosslinked systems. The modulation inscribed on azo-networks remains, to a certain extent, of about 30–40% of the initial modulation height at a temperature of up to 200 °C, around 85 °C over the film's bulk material T_g.

CONCLUSIONS

SRG generation was assessed on a series of epoxy-based azopolymers.

In the case of azo-prepolymers, the SRG formation process and its inscription rate turned out to be thickness-dependent. Patterns are formed faster in thicker samples, and, under a certain critical thickness, mass motion is prevented. The progressive erasure of the SRG with increasing temperature was observed, recovering the flat surface of the film as expected.

As regards SRGs formation in azo-networks, the process was satisfactory only for samples of at least 550 nm thick. The optimal conditions for SRG inscription on crosslinked films require at least one-micron thick sample, high power (approximately 200 mW cm^{-2}) and a minimum irradiation time of one hour. Under these irradiation conditions, no chromophore photoinduced degradation has been observed.

Tests conducted in networks with variable azobenzene content have shown that the formulations containing 25.8 wt % of chromophore ($r = 0.5$) present a significantly larger maximum height (123 ± 10 nm). Both the azo content and the network structure influence the maximum SRG amplitude that can be obtained.

When the azo-networks were subjected to a heating program, the only significant variation in modulation of the relief was observed at the T_g of the bulk material. Above this temperature (116 °C) and up to 200 °C, the relief modulation remained in about one third of the initial height, and did not completely disappear.

The obtained results are satisfactory and promising, providing a platform for the efficient formation of SRG directly from crosslinked polymers in a single step, in a reasonable time and to a significant extent.

ACKNOWLEDGMENTS

This work was supported by the following Argentinian institutions: Universidad Nacional de Mar del Plata (UNMdP), National Research Council (CONICET), and National Agency for the Promotion of Science and Technology (ANPCyT).

REFERENCES AND NOTES

1 M. Eich, J. H. Wendorff, *Makromol. Chem. Rapid Commun.* **1987**, *8*, 59.

2 K. Anderle, R. Birenheide, M. Eich, J. H. Wendorff, *Makromol. Chem. Rapid Commun.* **1989**, *10*, 477.

3 Z. Sekkat, M. Dumont, *Appl. Phys. B.* **1991**, *53*, 121.

4 P. Rochon, J. Gosselin, A. Natansohn, S. Xie, *Appl. Phys. Lett.* **1992**, *60*, 4.

5 A. Natansohn, P. Rochon, *Adv. Mater.* **1999**, *11*, 1387.

6 T. Ikeda, *J. Mater. Chem.* **2003**, *13*, 2037.

7 Z. S. Mahimwalla, K. G. Yager, J.-I. Mamiya, A. Priimagi, A. Shishido, C. J. Barrett, *Polym. Bull.* **2012**, *69*, 967.

8 Z. Sekkat, S. Kawata, *Laser Photon. Rev.* **2013**, 1.

9 A. Priimagi, A. Shevchenko, *J. Polym. Sci. Part B: Polym. Phys.* **2014**, *52*, 163.

10 H. Ishitobi, I. Nakamura, T. Kobayashi, N. Hayazawa, Z. Sekkat, S. Kawata, Y. Inouye, *ACS Photonics.* **2014**, *1*, 190.

11 A. Natansohn, P. Rochon, *Chem. Rev.* **2002**, *102*, 4139.

12 K. G. Yager, C. J. Barrett, *Curr. Opin. Solid State Mater. Sci.* **2001**, *5*, 487.

13 O. N. Oliveira Jr, L. Li, J. Kumar, S. K. Tripathy, In Photoreactive Organic Thin Films; Z. Sekkat, W. Knoll, Eds.; Elsevier Science: San Diego, **2002**; Chapter 14, pp. 430–486.

14 Z. Sekkat, *Appl. Opt.* **2016**, *55*, 259.

15 J. A. Delaire, K. Nakatani, *Chem. Rev.* **2000**, *100*, 1817.

16 N. K. Viswanathan, D. Y. Kim, S. Bian, J. Williams, W. Liu, L. Li, L. Samuelson, J. Kumar, S. K. Tripathy, *J. Mater. Chem.* **1999**, *9*, 1941.

17 P. S. Ramanujam, M. Pedersen, S. Hvilsted, *Appl. Phys. Lett.* **1999**, *74*, 3227.

18 S. K. Tripathy, N. K. Viswanathan, S. Balasubramanian, J. Kumar, *Polym. Adv. Technol.* **2000**, *11*, 570.

19 R. J. Stockermans, P. L. Rochon, *Appl. Opt.* **1999**, *38*, 3714.

20 J. Paterson, A. Natansohn, P. Rochon, C. L. Callender, L. Robitaille, *Appl. Phys. Lett.* **1996**, *69*, 3318.

21 J. P. Chen, F. L. Labarthet, A. Natansohn, P. Rochon, *Macromolecules* **1999**, *32*, 8572.

22 T. Fukuda, H. Matsuda, T. Shiraga, T. Kimura, M. Kato, N. K. Viswanathan, J. Kumar, S. K. Tripathy, *Macromolecules* **2000**, *33*, 4220.

23 C. J. Barrett, A. L. Natansohn, P. L. Rochon, *J. Phys. Chem.* **1996**, *100*, 8836.

24 C. J. Barrett, P. L. Rochon, A. L. Natansohn, *J. Chem. Phys.* **1998**, *109*, 1505.

25 N. Zettsu, T. Ubukata, T. Seki, K. Ichimura, *Adv. Mater.* **2001**, *13*, 1693.

26 W. Li, S. Nagano, T. Seki, *New J. Chem.* **2009**, *33*, 1343.

27 H. Takase, A. Natansohn, P. Rochon, *Polymer* **2003**, *44*, 7345.

28 J. Zhou, J. Yang, Y. Ke, J. Shen, Q. Zhang, K. Wang, *Opt. Mater.* **2008**, *30*, 1787.

29 A. B. Orofino, G. Arenas, I. A. Zucchi, M. J. Galante, P. A. Oyanguren, *Polymer* **2013**, *54*, 6184.

30 L. M. Sáiz, P. Ainchil, I. A. Zucchi, P. A. Oyanguren, M. J. Galante, *J. Polym. Sci. B Polym. Phys.* **2015**, *53*, 587.

31 X. Mai, R. S. Moshrefzadeh, U. J. Gibson, G. I. Stegeman, C. T. Seaton, *Appl. Opt.* **1985**, *24*, 3155.

32 K. G. Yager, C. J. Barrett, In Encyclopedia of NanoScience and NanoTechnology; H. S. Nalwa, S. Miyata, Eds.; CRC Press: Boca Raton, **2006**; Chapter 5, pp. 243–272.

33 L. M. Goldenberg, L. Kulikovsky, Y. Gritsai, O. Kulikovska, J. Tomczyk, J. Stumpe, *J. Mater. Chem.* **2010**, *20*, 9161.

34 O. Kulikovska, K. Gharagozloo-Hubmann, J. Stumpe, B. D. Huey, V. N. Bliznyuk, *Nanotechnology* **2012**, *23*, 485309.

35 K. G. Yager, C. J. Barrett, *J. Chem. Phys.* **2007**, *126*, 094908.

36 J.-A. He, S. Bian, L. Li, J. Kumar, S. K. Tripathy, L. A. Samuelson, *J. Phys. Chem. B.* **2000**, *104*, 10513.

37 C. J. L. Constantino, R. F. Aroca, J.-A. He, V. Zucolotto, L. Li, O. N. Oliveira, Jr, J. Kumar, S. K. Tripathy, *Appl. Spectrosc.* **2002**, *56*, 187.

38 T. M. Geue, A. G. Saphiannikova, O. Henneberg, U. Pietsch, P. L. Rochon, A. L. Natansohn, *Phys. Rev. E.* **2002**, *65*, 052801.

39 C. Cojocariu, P. Rochon, *Pure Appl. Chem.* **2004**, *76*, 1479.

40 A. Laventure, J. Bourotte, J. Vapaavuori, L. Karperien, R. G. Sabat, O. Lebel, C. Pellerin, *ACS Appl. Mater. Interfaces* **2017**, *9*, 798.